9th Latin American Congress in Heat and Mass Transfer
San Juan, Puerto Rico
October 20-22, 2002

PURE RADIATIVE HEAT EXCHANGE OF A THIN FIN

Federico Rossi , Franco Cotana
Dipartimento di Ingegneria Industriale, Università degli Studi di Perugia
via G. Duranti 1/A-4, 06125 Perugia (Italy).
e-mail: frossi@unipg.it
phone. +39 0755853846; fax +39 0755848470

ABSTRACT

An equation to evaluate pure radiative heat exchange of thin fins is proposed and analytically solved; equation solution may be conveniently employed to determine shadowed conditions thermal field of antennas, solar panels, tethered devices, remote controlled arms and heat dissipation systems on space facilities. Solution is compared to the results of a numerical simulation which has been carried out by means of a finite volumes code (Fluent); a good agreement has been found between simulated and analytical results. It is meant to verify the proposed method by an experimental setup which will be designed to be hosted on future space research mission.

1. INTRODUCTION

Classical relations which role the fin temperature distribution cannot be applied on system sited outside the earth atmosphere because of the absence of a heat and mass transport media [1]. Heat exchange occurs exclusively thank to radiative phenomenon. It is here proposed a new equation which roles the fin temperature distribution on pure radiative environment. The equation is conveniently simplified by some hypotheses which are sustainable outside the earth atmosphere in absence of direct solar radiation; thus an analytical solution was found adopting proper boundary conditions. The proposed equation and its solution were validated as it follows: two typical space fin structures were considered [2]; temperature distributions were found by the analytical solution; temperature distributions were also found by a numerical finite volume code; analytical and numerical results were compared. Comparison shows a good agreement between numerical and theoretical results for both two fin structures. The proposed equation may be employed to determine the "shadowed condition" thermal field of many space facilities like linear antennas, solar panels, remote controlled arms, tethered systems and nuclear engine heat exchangers. The analytical results will be validated by means of an experimental test which will be proposed to the main space agencies; it is expected to book such a test on an future research space program [3].

2. PURE RADIATIVE HEAT EXCHANGE EQUATION

2.1 HYPOTHESES

A single fin system reference scheme is shown in Fig. 1.

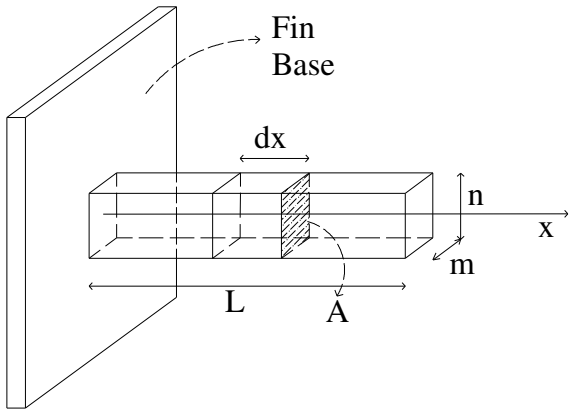

Fig. 1. Fin reference scheme.

In order to put down an equation for a stationary temperature distribution of a single fin, the following hypotheses were adopted:

- **A.** Fin base temperature T_0 is constant and uniform.
- **B.** Thermal conditions are stationary.
- **C.** Fin is soaked into a vacuum environment.
- **D.** Temperature depends on the only *x* spatial variable (see fig. 1); this hypothesis is more and more verified as:
  - thermal conductivity is higher and higher;
  - dimensions along *y* and *z* axes are

negligible with respect to the fin dimension along x axis (thin fin).

E. Fin cross section is constant.

F. The fin behaves as a gray body.

G. Outer space is black body in terms of radiative properties [4].

H. No direct radiation hits the fin (sun radiation) i.e. fin stands on a shadowed zone.

I. No heat exchanges between fin and fin base occurs; this hypothesis is supposed sustainable because of the following reasons:
- fin base temperature is comparable to the fin one with respect to the environment temperature;
- the "fin-base" F_{fw} view factor is generally very small with respect to the "fin-space" F_{fs} view factor [5].

J. According to hypothesis **G** space environment radiosity is not contributed by reflections terms [6].

K. No heat source is present along the fin.

L. According to hypothesis **I** the view factor F_{fs} is set 1.

M. Outer space radiative temperature T_a is approximately 3°K [4,7]; thus T^4_a is negligible with respect to $T^4(x)$.

N. Equation is solved by considering an infinite length fin.

2.2 EQUATION SOLUTION

Under **A**, **B**, **C**, **D**, **E**, **F**, **G**, **H**, **I**, **J**, **K** hypotheses the fin temperature distribution may be found by applying a heat flux rate balance at "x" generic section of the fin (see Fig.1):

$$\lambda A\frac{dT(x)}{dx}\bigg|_{x+dx} - \lambda A\frac{dT(x)}{dx}\bigg|_{x} = PF_{fs}\sigma_0\varepsilon\left[T^4(x) - T_a^4\right]dx \qquad (1)$$

By considering hypotheses **I** and **M** eq.(1) becomes:

$$\frac{d^2T(x)}{dx^2} = k^2T^4(x) \qquad (2)$$

where:

$$k = \sqrt{\frac{P\sigma_0\varepsilon}{\lambda A}} \qquad (3)$$

Eq. (2) may be rewritten as follows [8]:

$$2\,T'(x)\frac{dT'(x)}{dx} = 2\,k^2\,T^4(x)T'(x) \qquad (4)$$

with:

$$T'(x) = \frac{dT(x)}{dx} \qquad (5)$$

Thus the following identity is attained:

$$\frac{dT'(x)^2}{dx} = 2k^2T^4(x)T'(x) \qquad (6)$$

Solving eq. (6) with respect to $T'(x)$ we have:

$$T'(x) = \pm\sqrt{\frac{2}{5}k^2T^5(x) + C_1} \qquad (7)$$

A closed form solution of eq. (7) may be found by observing hypothesis **N**, according to which $T(x\to\infty)$ is to be zero and, consequently, heat flux $-\lambda AT'(x\to\infty)$ must also be zero. In order to achieve the previous statements, C_1 must be zero too;

According to hypotheses **H**, **K** and **M**, temperature must be a monotonic descending function with respect to x variable; thus the following condition must be verified:

$$T'(x) \le 0 \qquad (8)$$

According to eq. (8), the only physically admitted solution of eq. (7) must be found just by solving:

$$T'(x) = -\sqrt{\frac{2}{5}k^2T^5(x)} \qquad (9)$$

By integrating eq. (9), we have:

$$T(x) = k^{-\frac{2}{3}}\left(\frac{10}{9}\right)^{\frac{1}{3}}(x + C_2)^{-\frac{2}{3}} \qquad (10)$$

C_2 assumes two different values by the peculiar boundary condition which is taken into account. The following are two possible boundary conditions:

α. for $x = 0$, $T(0) = T_0$;

β. for $x = 0$, $-\lambda\frac{dT(x)}{dx}\bigg|_{x=0} = q_0$

q_0 is a given heat flux per unit of area. Eq. (11) and eq. (12) give the values of C_2 which are

alternatively obtained by applying α and β conditions in equation (10):

$$C_2 = k^{-1}\left(\frac{10}{9}\right)^{\frac{1}{2}} T_0^{-\frac{3}{2}} \tag{11}$$

$$C_2 = \left(\frac{2}{3}\lambda\right)^{\frac{3}{5}} \left(\frac{10}{9}\right)^{\frac{1}{5}} k^{-\frac{2}{5}} q_0^{-\frac{3}{5}} \tag{12}$$

Let's write the fin temperature distribution (see eq. (13)) for the only temperature boundary condition (condition α):

$$T(x) = k^{-\frac{2}{3}}\left(\frac{10}{9}\right)^{\frac{1}{3}} \left(x + k^{-1}\left(\frac{10}{9}\right)^{\frac{1}{2}} T_0^{-\frac{3}{2}} \right)^{-\frac{2}{3}} \tag{13}$$

3. FIN EFFICIENCY

Fin efficiency (see eq.(14)) is defined as the ratio between the effective heat rate exchanged by the fin and the heat rate exchanged by a uniform temperature fin [1]:

$$\eta = \frac{q_{eff}}{q_{\max}} \tag{14}$$

The effective heat flux exchanged by fin is:

$$q_{eff} = \int_0^L P\varepsilon\sigma_o T(x)^4 dx \tag{15}$$

According to the hypotheses of paragraph 1, heat flux exchanged by a uniform temperature fin is:

$$q_{max} = PL\sigma_0 \varepsilon T_0^4 \tag{16}$$

In base to the above definition fin efficiency becomes:

$$\eta = \frac{3}{5}\left(\frac{10}{9}\right)^{\frac{4}{3}} T_0^{-4} k^{-\frac{8}{3}} L^{-1} \left[T_0^{\frac{5}{2}} k^{\frac{5}{3}} \left(\frac{10}{9}\right)^{-\frac{5}{6}} + \right.$$
$$\left. - \left(L + T_0^{-\frac{3}{2}} k^{-1} \left(\frac{10}{9}\right)^{\frac{1}{2}} \right)^{-\frac{5}{3}} \right] \tag{17}$$

Eq. (17) can be rewritten (see eq. (18)) in terms of an adimensional parameter :

$$\eta = \frac{1}{s}\left[\sqrt{\frac{2}{5}} - \frac{3}{5} \cdot \left(\frac{10}{9}\right)^{4/3} \cdot \left(s + \sqrt{\frac{10}{9}} \right)^{-5/3} \right] \tag{18}$$

where *s* is adimensional:

$$s = k \cdot L \cdot T_o^{3/2} = \sqrt{\frac{P\sigma_0\varepsilon \cdot L^2 \cdot T_o^3}{\lambda \cdot A}} \tag{19}$$

In Fig. 2 fin efficiency versus *s* is sketched. It may be observed that fin efficiency decrease with *s* which means that fin efficiency decrease when fin length, *k* parameter and fin base temperature increase.

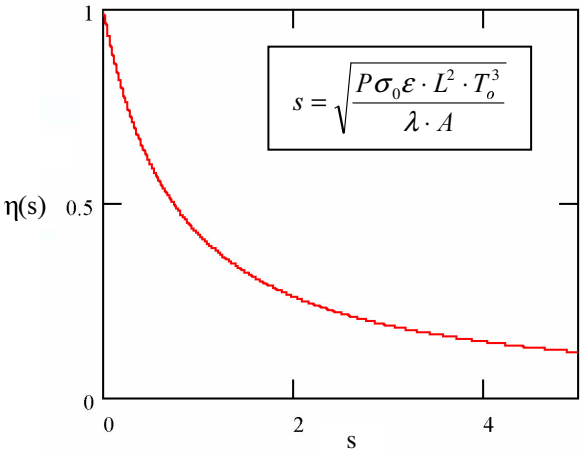

Fig. 2. Fin efficiency versus *s*

By observing eq. (14) fin heat flux rate exchanged by the fin may be simply calculated as follows:

$$q_{eff} = \eta \cdot \sigma_o \cdot \varepsilon \cdot P \cdot L \cdot T_o^4 \tag{20}$$

4. NUMERICAL SIMULATIONS AND COMPARISON

4.1 TYPICAL GEOMETRICAL STRUCTURES FOR SPATIAL APPLICATIONS

Two different cases are taken into account to compare the temperature distributions supplied respectively by a numerical simulation and by the proposed analytical relation:

CASE **A**: planar structure (Fig. 3.a);

CASE **B**: line structure (Fig. 3.b).

Both cases constitute typical structures for spatial applications since many space craft peripheral devices are geometrically characterized by the mentioned

shapes [9]: linear antennas, tethered systems, solar panels, remote controlled arms and screening systems.

Both structures are characterized by the same material properties: λ = 200 W/mK, ε=0.5, ε=0.3. Such properties corresponds to aluminium alloy with two different surface coating [10]. The planar structure is characterized by parallelepiped shape the dimensions of which are: L=2m, W=1m, H=0.01m [11]. The line structure is circular-cross cylinder the dimensions of which are D=0.01m, L=1m [11].

In Fig. 3 planar and line structures are sketched.

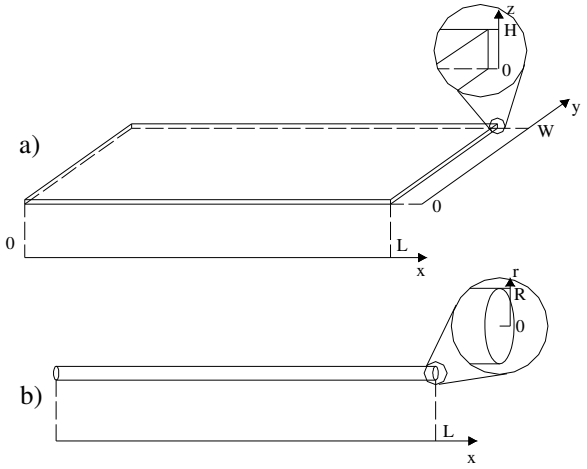

Fig. 3. a) planar structure; b) line structure.

4.2 NUMERICAL SIMULATIONS

Cases **A** and **B** temperature distributions and heat flux rates were simulated by means of a "finite volume" numerical code [12].

Simulations have been carried out by meshing the structures and the environment they are soaked in as follows:

CASE **A**. the planar structure was divided in about 30000 hexaedrical cells. A cubic vacuum volume was built all around the structure. The vacuum volume was meshed in about 25000 hexaedrical cells.

CASE **B**. the line structure was divided in about 40000 tetrahedral cells. A vacuum volume surrounding the structure was meshed in about 30000 tetrahedral cells.

The above structures discretisations were made automatically by the code in order to get both convergence and a temperature accuracy which is set by the following criterion: when temperature variation between two consecutive iterations is lower than 0.05°K iteration process is halted [12].

Simulations were made by applying the following boundary conditions:

- fin base temperature was set 300°K;
- mass transport phenomena were cut off;
- only radiative heat exchanges were considered;
- the vacuum temperature was set 3°K.

4.3 RESULTS COMPARISON

The analytical formula (see eq.(13)) of temperature distribution was applied to CASE **A** and CASE **B**.

Heat flux rates were determined for both cases by substituting fin efficiency (see eq.(18)) on eq.(14).

In Figg. 4, 5 CASE **A** simulated and analytical temperature distributions are sketched for respectively ε = 0.5, ε = 0.3.

In Figg. 6, 7 CASE **B** simulated and analytical temperature distributions are sketched for respectively ε = 0.5, ε = 0.3.

Simulated temperature sketched in Figg. 4 and 5 are shown for z=H and y=W/2 (plate surface); simulated temperature sketched in Figg. 6 and 7 are shown for r=R (line structure surface).

However, as discussed in paragraph 4.3, very small temperature non uniformities were found along transversal axes (y and z for CASE A, r for CASE B); thus the previous representations may be considered the same for any value of y, z and r.

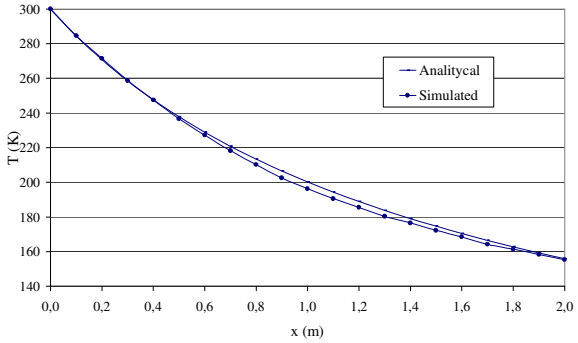

Fig. 4. Simulated temperature distribution: CASE A, ε = 0.5.

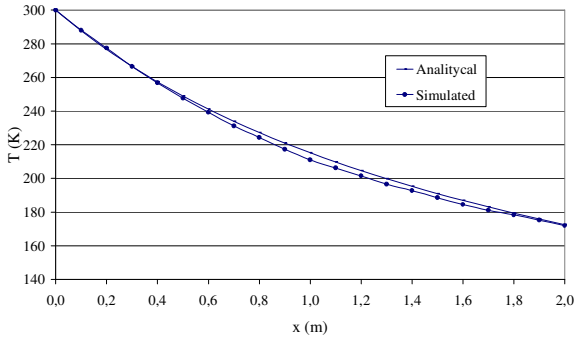

Fig. 5. Simulated temperature distribution: CASE A, ε = 0.3.

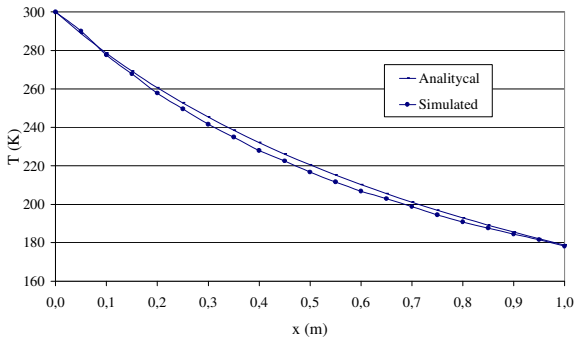

Fig. 6. Simulated temperature distribution: CASE B, $\varepsilon = 0.5$.

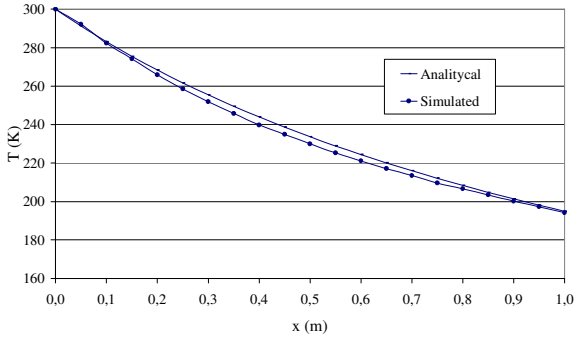

Fig. 7. Simulated temperature distribution: CASE B, $\varepsilon = 0.3$.

It may be observed that simulated temperatures are very close to analytical ones for each case. In Tab.1 simulated and analytical fin efficiency and heat flux rate are reported.

A comparison between simulated and analytical results is shown in Tab. 2: temperature comparisons are made in terms of relative maximum temperature difference with respect to analytical value; heat flux rate comparisons are made in terms of relative heat flux rate difference with respect to analytical value.

For each case and for both values of ε the differences between simulated and analytical results are very small: maximum temperature difference is **2.0%** and maximum heat flux rate difference is **2.7%**.

Tab. 1. Simulated and analytical fin efficiency and heat flux rates.

Case	ε	η		q_{eff} [W]	
		Analytical	*Simulated*	*Analytical*	*Simulated*
A	*0.5*	0.29	0.28	268.64	265.21
	0.3	0.35	0.34	193.59	190.37
B	*0.5*	0.37	0.36	2.68	2.61
	0.3	0.43	0.42	1.88	1.83

Tab. 2. Comparison between simulated and analytical fin efficiency and heat flux rate.

Case	ε	ΔT_{max} [%]	Δq_{eff} [%]
A	*0.5*	2.0	1.3
	0.3	1.9	1.7
B	*0.5*	1.8	2.6
	0.3	1.7	2.7

4.3 HYPOTHESES DISCUSSION

The assumption of **G**, **H**, **I**, **J**, **L**, **M** hypotheses should determine a lower temperature than the effective one all fin through; however it is not verified by the numerical simulations: it makes suppose that **N** hypothesis produces an opposite trend on temperature distribution with respect to the adoption of the mentioned **G**, **H**, **I**, **J**, **L**, **M** hypotheses.

A test of hypothesis **D** may be carried out observing the simulated temperature distributions along *y* and *z* axes at fin final section where temperature non uniformities are maximum.

In Figg. 8a and 8b, CASE A (ε=0.5) temperature distribution at x=L along respectively *y* and *z* axes is sketched. In Fig. 9, CASE B (ε=0.5) temperature distribution at x=L along *r* axis is sketched.

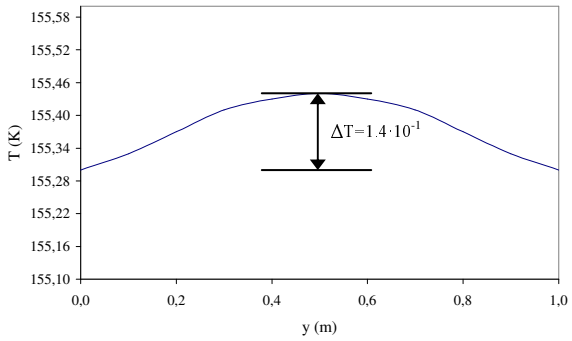

(a)

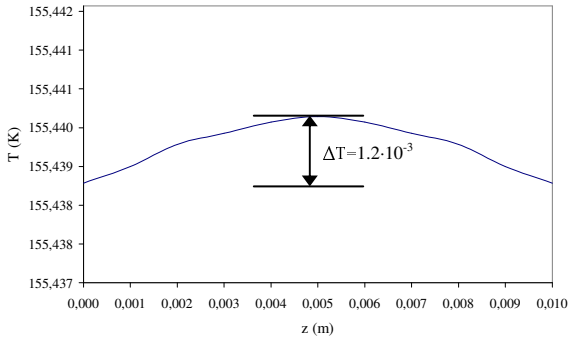

(b)

Fig. 8. a) Temperature distribution along y axis; b) Temperature distribution along z axis CASE A, $\varepsilon = 0.5$, x=L

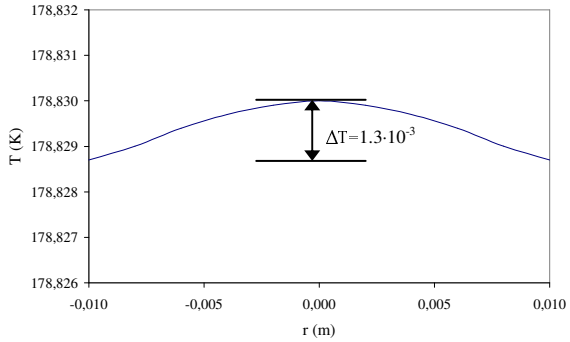

Fig. 9. Temperature distribution along r axis; CASE B, $\varepsilon = 0.5$, x=L

It may be observed (see figg. 8 and 9) that maximum temperature difference is 0.14°K which occurs for CASE A along *y* axis. The very small values of temperature differences on transversal axes make hypothesis **D** sustainable.

A test of hypothesis **M** may also be carried out by calculating the fin heat flux rate as follows:

$$q_{eff} = -\lambda A \left.\frac{dT(x)}{dx}\right|_{x=0} \tag{21}$$

According to hypothesis **N,** if temperature distribution of eq. (13) is employed to calculate eq. (21), an infinite length fin flux rate is attained:

$$q_{\infty} = \left(\frac{2}{5}\right)^{\frac{1}{2}} \lambda A\, k T_0^{\frac{5}{2}} \tag{22}$$

Eq. (22) flux rate is *L* insensitive and verifies the following three terms identity:

$$q_{\infty} = \left(\frac{2}{5}\right)^{\frac{1}{2}} \lambda A\, k T_0^{\frac{5}{2}} = \lim_{L\to\infty} \int_0^L P\varepsilon\sigma_o T(x)^4\, dx = \\ = \lim_{L\to\infty} \eta(s(L)) \cdot PL\varepsilon\sigma_o T_o^4 \tag{23}$$

Heat flux rate of an infinite length fin may also be achieved regardless hypothesis **M**, by which eq.(2) becomes:

$$\frac{d^2T(x)}{dx^2} = k^2 \left(T^4(x) - T_a^4(x)\right) \tag{24}$$

Eq. (24) may be solved in terms of temperature first degree derivative by applying the same method employed to solve eq. (2). Thus, we have:

$$T'(x) = \frac{dT(x)}{dx} = -\sqrt{\frac{2}{5}k^2T^5(x) - 2k^2T_aT(x)} \tag{25}$$

Heat flux rate may be obtained by observing that eq. (25) is proportional to heat flux rate:

$$q_{a\infty} = -\lambda A T'(x)\Big|_{x=0} = \lambda A k \sqrt{\frac{2}{5}T_o^5 - 2T_a^4T_o} \tag{26}$$

Hypothesis **M** is certainly sustainable because eq. (27) is very close to unit when T_a is smaller than T_o:

$$\frac{q_{a\infty}}{q_{\infty}} = \sqrt{1 - 5\cdot\left(\frac{T_a}{T_o}\right)^4}\ . \tag{27}$$

Anyway the agreement between analytical and simulated results suggests that the set of hypotheses adopted to formulate and to solve eq. (2) is globally sustainable.

5. CONCLUSIONS

The equation which governs the temperature distribution along a one dimensional fin which is soaked into outer space environment was introduced; a solution was also found by adopting simplifying hypotheses. Fin efficiency was determined which depends on an adimensional parameter. A numerical simulation was carried out in order to predict temperature distribution and flux rate of two typical geometrical structures employed in spatial devices: a line structure (antennas, mechanical arms, tethered systems) a planar structure (solar panels, screening systems). The proposed analytical solution was also applied to the previous two typical structures; a comparison between numerical and analytical results was made: a quite small difference was found both on temperature distribution and on flux rate (maximum flux rate difference is 2.7 %). The numerical simulation results allow to state that the mentioned simplifying hypotheses were sustainable.

An experimental test will validate the analytical results; the test will be achieved by realizing a custom facility which needs to be installed into an outer space environment. Many queries are actually going to be made to the most important world space agencies in order to book the test for a future spatial research mission.

6. LIST OF SYMBOLS

Symbol	Unit	Description
A	m^2	Cross-section area
C_1	$m^{-2}K^2$	Integration constant
C_2	m	Integration constant
F_{fw}	Adimensional	Fin-Base view factor
F_{fs}	Adimensional	Fin-Space view factor
k	$m^{-1}K^{-3/2}$	Material properties parameter
H	m	Fin height (CASE **A**)
L	m	Fin length
P	m	Cross-section perimeter
q_{eff}	W	Effective heat flux
q_{max}	W	Heat flux exchanged by a uniform temperature fin
q_{∞}	W	Heat flux exchanged by an infinite length fin
$q_{ax\infty}$	W	Heat flux exchanged by an infinite length fin regardless hypothesis **M**
q_0	W/m^2	Given heat flux
R	m	Fin section radius (CASE **B**)
r	m	Fin section radial reference axis (CASE **B**)
s	Adimensional	Adimensional parameter
$T(x)$	K	Temperature distribution
T_a	K	Space radiative temperature
T_0	K	Fin base temperature
x	m	Fin longitudinal reference axis
W	m	Fin width (CASE **A**)
y	m	Fin transversal reference axis (CASE **A**)
z	m	Fin transversal reference axis (CASE **A**)
ΔT_{max}	Adimensional (%)	relative maximum difference between simulated and analytical temperature distribution
Δq_{eff}	Adimensional (%)	relative difference between simulated and analytical heat flux rate
ε	Adimensional	Emissivity
η	Adimensional	Fin efficiency
λ	W/mK	Conductivity
σ_0	W/m^2K^4	Stefan-Boltzmann constant

7. BIBLIOGRAPHY

[1] Kreith, F., 1998, "Principles of heat transfer", Wadsworth Publishing Company;

[2] Fortesque, P., Stark, J., 1995, "Spacecraft Systems Engineering", John Wiley and Sons;

[3] http://props.oss.hq.nasa.gov, "Office of Space Science Proposal";

[4] Tascione, T., 1988, "Introduction to the Space Environment", Orbit Book Co.;

[5] Kivelson, M., Russell, C.T., 1995, "Introduction to Space Physics", Cambridge University Press;

[6] Jursa, A.S., 1985, "Handbook of Geophysics and the Space Environment", Air Force Geophysics Laboratory, Hanscom AFB;

[7] Tribble, A., 1995, "The Space Environment", Princeton University Press;

[8] Vinti, C. 1989, "Lezioni di analisi matematica", vol.2, Galeno Editrice, Perugia;

[9] Meyer, X., 1999, "Elements of Space Technology", Academic Press;

[10] Nayar, A., 1997, "The Metal Databook", McGraw-Hill;

[11] Pisacane, V.L., Moore, R.C., 1994, "Fundamentals of Space Systems", Oxford University Press;

[12] Fluent Incorporated, 1998, "Fluent 5 user guide".

8. ACKNOWLEDGMENT

The authors thank Dr. Andrea Nicolini for the precious collaboration.